

INVESTIGATION OF METALLURGICAL AND MICROHARDNESS PROPERTIES OF TITANIUM ALLOY IN LASER METAL DEPOSITION PROCESS

Mahamood R.M.^{1,*}, Abdulkareem S.¹, Ajao K.R.² and Aweda J.O.¹

¹Department of Mechanical Engineering, University of Ilorin, Nigeria.

²Department of Materials and Metallurgical Engineering, University of Ilorin, Nigeria

*Corresponding Author Email address: mahamoodmr2009@gmail.com

ABSTRACT

This paper reports on the investigation of metallurgical and microhardness properties of laser metal deposition of Titanium alloy- Ti-6Al-4V. Ti-6Al-4V substrate and Ti-6Al-4V powder (150-200 μm) both at 99.6% purity were used in this study. The input laser power varied between 0.8 and 4.0 kW while other processing parameters were kept constant. They include the scanning speed of 0.005 m/sec, powder flow of 1.44 g/min and the gas flow rate of 4 l/min. The microstructure and the microhardness were examined under the optical and scanning electron microscope. The microhardness was measured using the Vickers hardness tester. The study revealed that the layer band occurred in all the samples except those samples at very high laser powers. The microstructure of the heat affected zone is characterized with fine globular primary alpha and beta grains at low laser power and become coarse as the laser power was increased. The microhardness was found to initially increase and then decrease as the laser power was increased beyond 3 kW.

Keywords: Metal Deposition Process, Laser power, Macroscopic Banding, Microhardness, Microstructure.

INTRODUCTION

One of the most produced and commonly used alloy materials in aerospace sector is Titanium Ti-6Al-4V alloy (Esmailian and Mehrvar (2007); Peters et al (2003)). This is because of its good structural stability and corrosion resistance at elevated temperature (Cai et al (1999); Lu et al. (2012); Mathew and Donachai (1988)). However, Titanium alloy is one of difficult-to-machine materials because of its poor thermal response at high temperature which results in drastic reduction in tool life during machining (Wang and Ezugwu (1997)). In order to offset or minimize the problem encountered during machining of this material, a non-traditional machining process is required. One of the non-traditional machining techniques that can be used is Additive Manufacturing (AM) process. AM technique processes material through addition of materials (powder) in layers by layers (Mazumda and Song 2010)). The main AM technique is Laser Metal

Deposition (LMD) that produces solid components from CAD model file (Toyserkani and Khajepour (2006); Wu et al. (2004)).

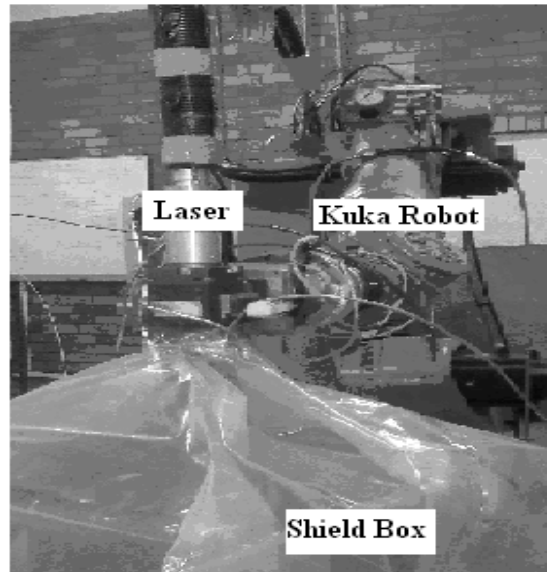
The LMD can be used to carry out repair of high valued component parts that were discarded and can equally be used to produce functionally graded materials because of its ability to handle different materials (Pinkerton et al. (2008); Mahamood et al. (2012)). This process is very suitable for the production of aerospace parts because it increases fly-to-buy ratio and repair of high valued components can readily be achieved in situ with LMD (Brandl et al. (2011); Kobryn and Semiatin (2000); Bergan (2000); Cottam and Brandt (2011)). LMD process is achieved by feeding powder into the melt pool that is generated by sharply focused collimated laser beam on the substrate. The melt pool is generated by the interaction between the substrate and the laser.

Among the many researchers that have carried out LMD on Ti-6Al-4V alloys and other materials with different LMD input parameters are: Lu et al (2012); Brandl et al (2011) and Kobryn (2000). Processing parameters are found to have significant influence on the evolving properties (Mahamood et al. (2013a); Mahamood et al. (2014); Mahamood et al. (2016)). Controlling a single variable is much more simpler in the development of a closed loop control system than using combination of variables which becomes more complex especially where interactions exists between these variables.

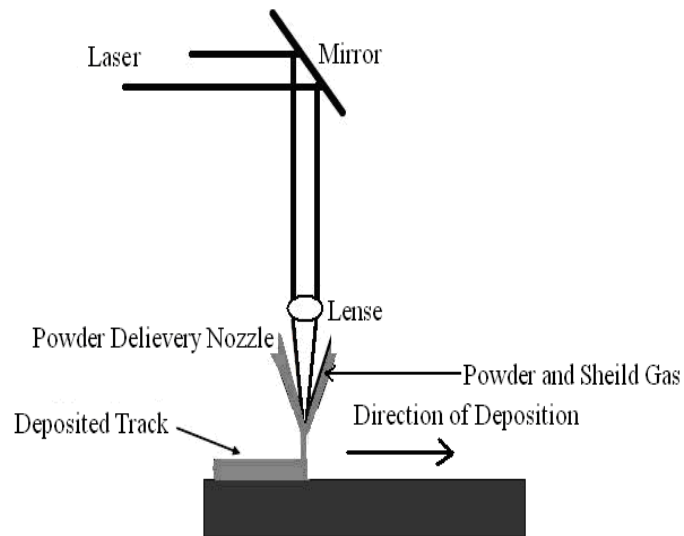
The present study is to investigate the effect of laser power on the microstructure and the microhardness of Ti-6Al-4V with. The objective of the study is to help ease the difficulty of developing a close loop control system for full automation of the laser metal deposition process. That is, by controlling only one process parameter such as laser power will help to simplify close loop control system design which will use the laser power control to achieve metallurgical as well as microhardness properties control. This is particularly useful in the repair process.

EXPERIMENTAL TECHNIQUE

A 4.4 kW fiber delivered Nd-YAG laser with coaxial powder nozzles was used to carry out the LMD process in this study. Manipulation of laser arm and powder nozzles as well as control of the process was carried out by a Kuka robot attached to the machine, while shielding of the deposit was achieved by the use of plastic material (Figure 1a). The gas assisted powder was delivered into the melt pool created by the laser on the substrate in order to generate a deposited track. The schematic of the deposition process is shown in Figure 1b.



(a)



(b)

Figure 1: (a) Experimental setup (b) Schematic of Laser Metal Deposition Process

A 99.6% pure Ti6Al4V substrate (72 x 72 x 5 mm) plate and pure Ti6Al4V powder (150 to 200 μm) were used during the LMD process. A preliminary experiment to establish a process window that produces fully dense, pore free and good metallurgically bonded deposit was carried out. From the result of the preliminary experiment, a laser power of 800 W, scanning speed of 0.005 m/sec,

powder flow rate of 1.44 g/min and a gas flow rate of 4 l/min were the LMD input parameters that satisfied the conditions of a fully dense, pore free and better metallurgical bonded deposit. The resulting input parameters with the variation of laser power between 0.8 and 4.0 kW were used for the second LMD process. The process parameters (Table 1), with scanning speed of 0.005 m/sec, powder flow rate at 1.44 g/min and gas flow rate of 4 l/min were used for the deposition.

Table 1: Processing parameters

Sample Designation	Laser Powers (kW)
A	0.8
B	1.2
C	1.6
D	2.0
E	2.4
F	2.8
G	3.0
H	3.4
I	3.8
J	4.0

The substrate was cleaned by sand blasting and application of acetone solution before LMD process. Track length of 60 mm was deposited for each of the processing parameter and designated as A to G. The samples were laterally sectioned and mounted in resin after the deposition process. Grinding, polishing and etching of the samples were carried out in accordance to the standard metallographic preparation of Titanium. The samples were examined under Optical Microscopy (OM). The microhardness was performed using the Vickers hardness tester with a load of 500 g and a dwelling time of 15 seconds with spacing between the indentations fixed at 15 μ m.

RESULTS AND DISCUSSION

Figure 2 shows the microstructure of the Ti-6Al-4V substrate used as observed under the optical microscope, while the macrograph of the Ti6Al4V powder is shown in Figure 3. The particle size distribution of the powder is shown in Figure 4. The microstructure (Fig. 2) is characterized by alpha and beta grain structure with the lighter part showing the alpha grains and the darker parts showing the beta grains. The powder is gas atomized and spherical in shape. The particle size distribution is Gaussian in nature (Fig. 4).

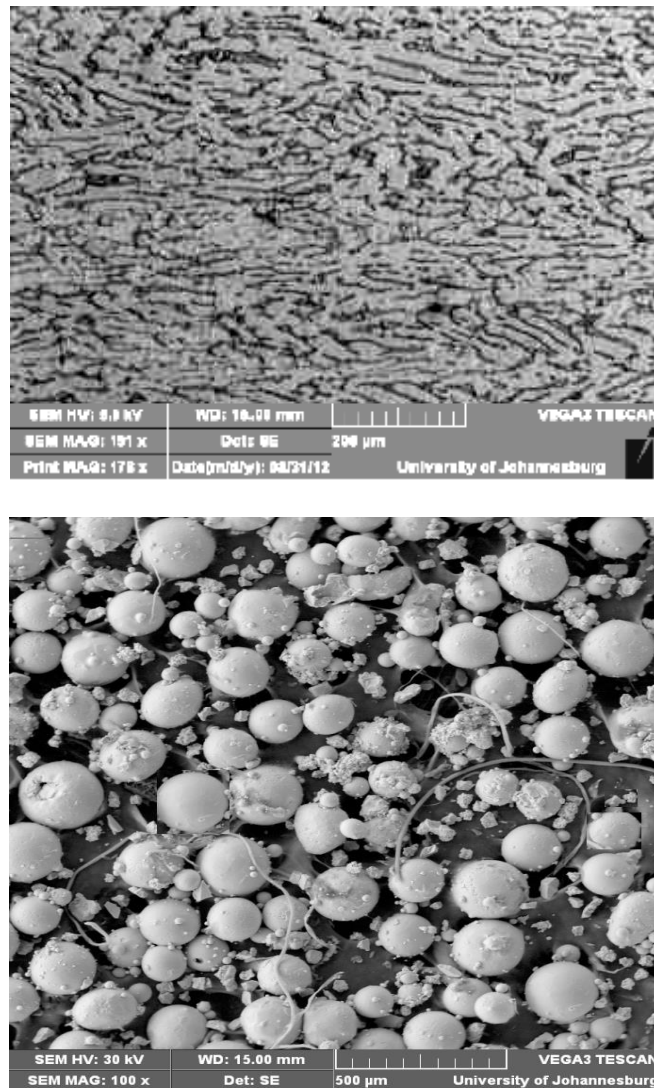


Figure 3: Morphology of the Ti6Al4V powder

The schematic of the deposit as viewed from the cross-section is shown in Figure 5, it is divided into three zones. The Deposit Zone (DZ) consists of the melted deposited powder, the Fusion Zone (FZ) consists of the mixture of the substrate material and the deposited powder. The Heat Affected Zone (HAZ) is the substrate material which act as a heat sink that received highest heat to cause microstructural changes. The experimental results are divided into two parts namely: 1. the macrostructure / microstructural analysis and 2. microhardness results.

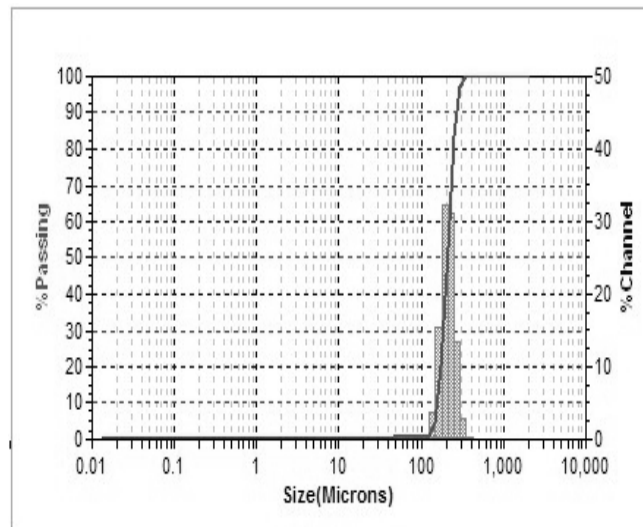


Figure 4: Particle size analysis of the Ti6Al4V powder

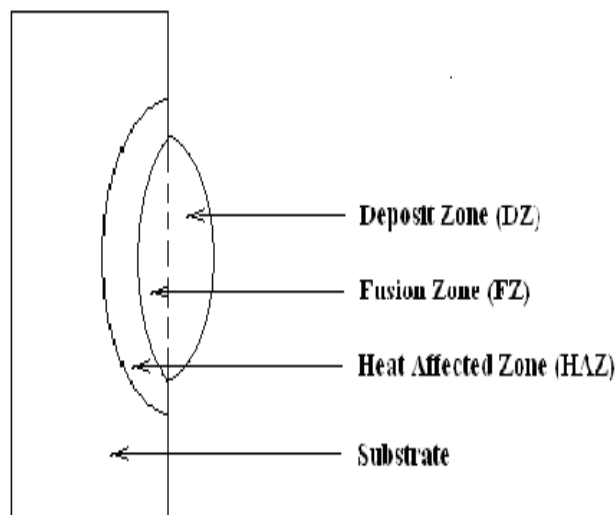


Figure 5: Schematic of the cross sectional view of deposit on the substrate (Mahamood et al. (2013b))

3.1 Morphology and Microstructure

The morphology of the sample A is shown in Figure 6 displaying the deposit zone, the fusion zone and the heat affected zone as depicted by the Figure 5. It can be observed that the grains are continuous from the fusion zone to the deposit zone and are columnar in nature, this is seen in all the samples. Figure 7a and 7b show

the sample A and sample F respectively indicating the macroscopic banding that was observed in all the samples. The globular grains shown in Figure 7 a to 7c is seen to change from fine to coarse as the laser power was increased. The globular grains in Figure 7c are bigger because of the very high power that resulted in larger grain growth due to longer solidification rate.

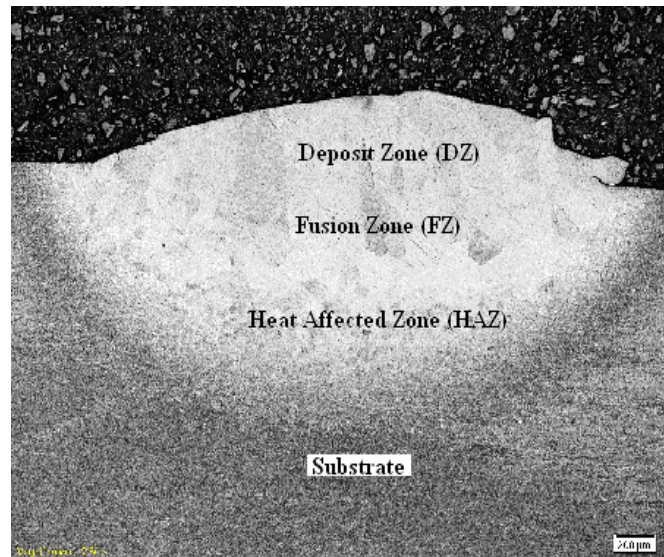
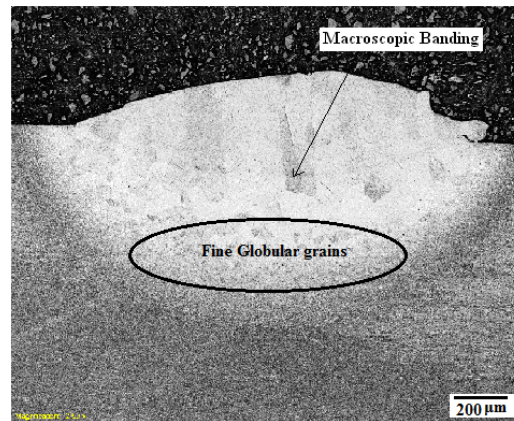
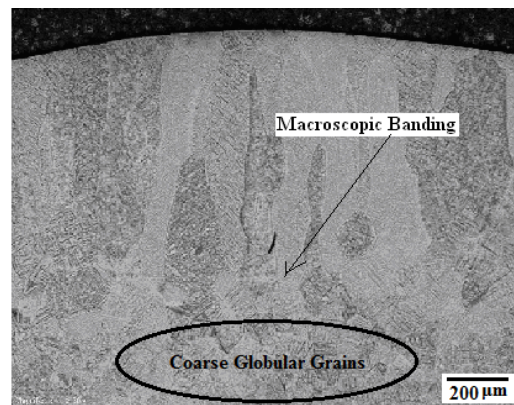


Figure 6: Morphology of Sample A showing the different zones

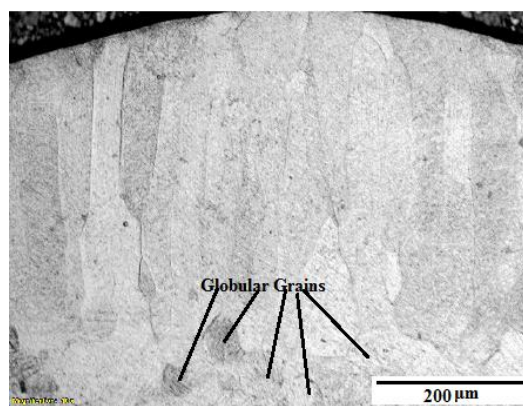
The macroscopic observation (Figure 6) revealed that the deposit zone and the fusion zones were characterised by continuous columnar prior β grains, this is the characteristics of Ti6Al4V when casted or laser deposited (Brandl et al. (2011); Kobryn and Semiatin (2003)). It is worthy to note that the macroscopic banding shown in Figures 7a and 7b are observed in all the samples produced up till 3.0 kW. The samples produced at higher laser power does not show this macroscopic banding. This is different from what was reported in the literature that the macroscopic banding was only common to multi - layer deposits (Kobryn and Semiatin (2003)). These banding are often attributed to reheat of the previous layer by the succeeding layer thereby creating another heat affected zone (Kobryn and Semiatin (2003)).



(a)



(b)



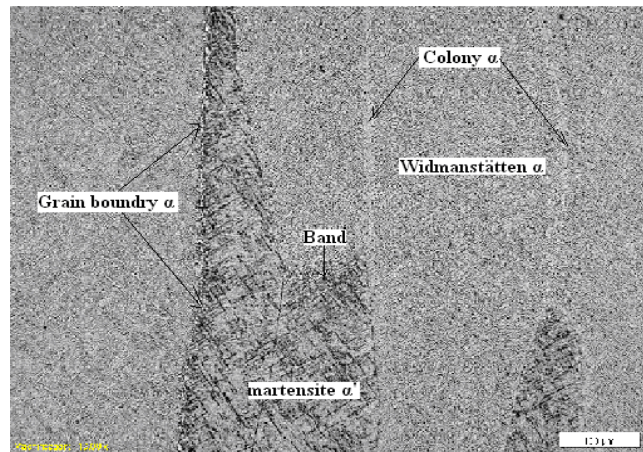
(c)

Figure 7: Micrograph showing Macroscopic banding of (a) sample A (b) Sample F and (c) sample J showing coarser globular grains

Only single layer was deposited for each of the processing parameter in this study and yet these bands were observed in most of the samples. It can be inferred that these banding were not as a result of reheating of the layer but could be attributed to the interaction in the fusion zone. The fusion zone must have experienced some kind of shrinkage during solidification as a result of mixing action that takes place and much more rapid solidification. The samples at laser power beyond 3 kW did not show macroscopic banding and this could be attributed to much slower solidification rate as a result of larger melt pool created at larger laser power. The slower solidification rate help to eliminate the shrinkage that was attributed to the cause of macroscopic banding at much lower laser power. Figure 8 shows the microstructure of sample G indicating the various alpha grains and the microstructure at the band area. It can be observed that change in the microstructure of the band area is localised (Figure 8) to a particular grain which further explains that this could be due to shrinkage in this location as a result of gas escape during solidification of the fusion zone as all the bands are present in the fusion zone.

Figure 9 and Figure 10 shows the macrographs of the fusion and the heat affected zone of the samples B and D respectively. The grain growth in the deposit zones in all the samples are dominated by heterogenous nucleation; this is because the substrate material is the same as the powder material (Messler (1999)) and they grow epitaxially on the globular grains in the HAZ (Kou (1987)) as seen in Figure 9 and Figure 10. The crystals at the fusion zone builds on the globular grains of the heat affected zone (see Figure 9 and 10) as observed in all the samples and the population of the globular grains in the heat affected zone decreases with increase in the laser power. This is because the cooling rate decreases as the laser power increases, which results in less nucleation sites and also the melt pool stays longer on the substrate before it completely solidifies.

The longer time spent by the melt pool results in more grain growth in the heat affected zone, i.e more grains were merged together. This also translate to the fewer number of columnar grains in the deposit zone as the laser power increases because the columnar grains grow epitaxially on the globular grains in the HAZ of the substrate.



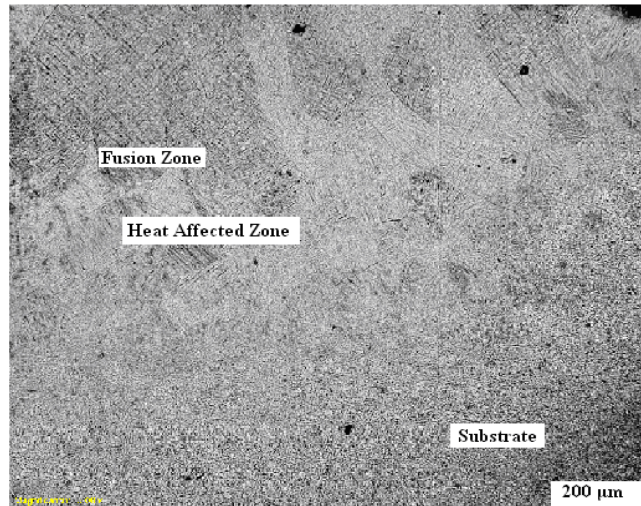
(a)



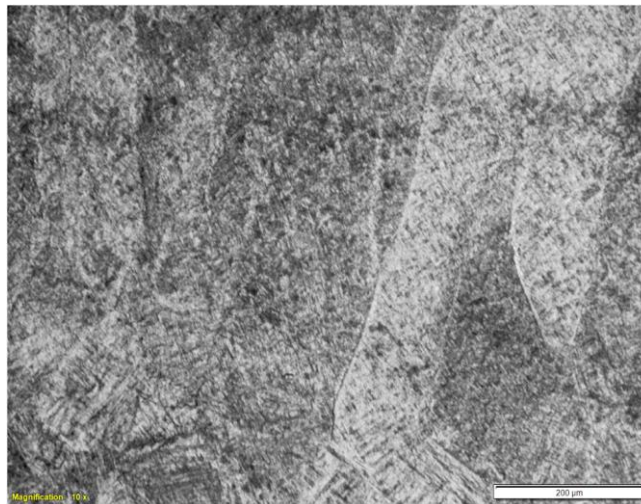
(b)

Figure 8: (a) Microstructure of the fusion zone of Sample G showing different α grains
(b) Higher magnification of the (a)

The direction of the grain growth is opposite the maximum temperature gradient. The maximum temperature gradient is towards the substrate (heat sink), hence the grain growth direction is opposite this direction. The microstructure of the deposit zone of samples C and D are shown in Figure 11a and 11b respectively. The microstructures of the heat affected zones of the samples A, C and G are shown in Figure 10 and is characterised by acicular alpha grain structure.



(a)



(b)

Figure 9: (a) Macrographs of fusion zone and the heat affected zone of sample B
(b) Higher magnification of Figure 9 (a)

3.2 Microhardness

Figure 13 shows the average microhardness values of all the samples showing the relationship between changes in average microhardness and the changes in laser power. The average hardness value of each of the sample was determined and plotted against the sample designation. The best line of fit was drawn across the

points to see the trend as shown in Figure 13. The substrate material has the lowest average microhardness value.

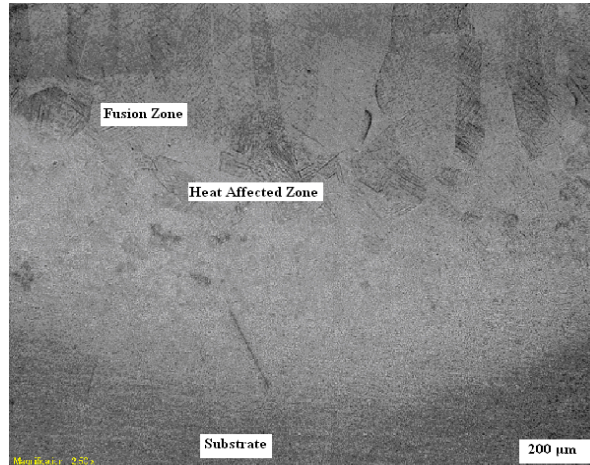


Figure10: Macrographs of fusion zone and the heat affected zone of sample D

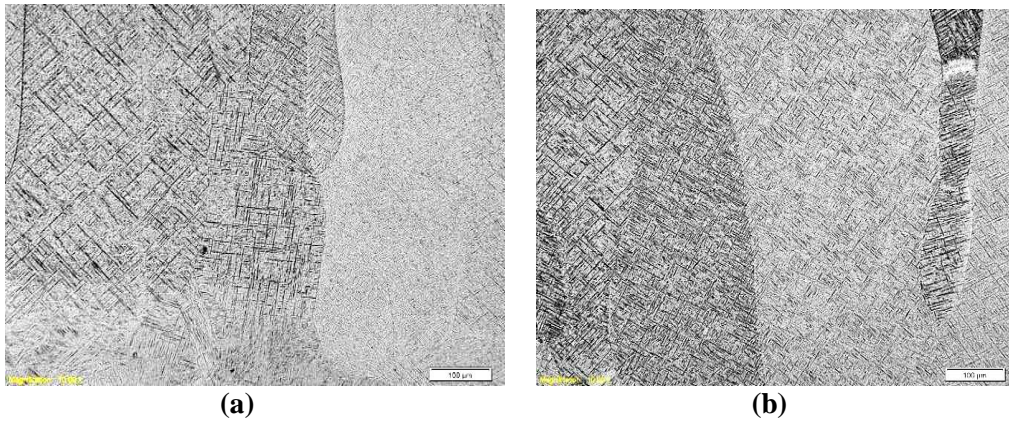


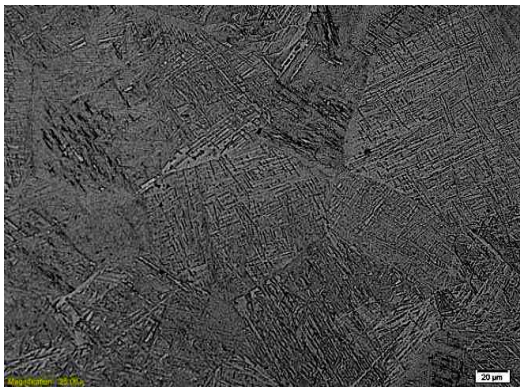
Figure 11: Microstructure of the deposit zone of (a) Sample C (b) Sample D

It was observed that the average Vickers hardness value increases with increase in the laser power up till the laser power of 3 kW and began to decrease as the laser power was further increased. The initial increase in microhardness as the laser power was increased was as a result of microstructural changes from fine martensitic structures to coarser martensitic structure as the laser power increases. The solidification rate at laser power of 3 kW and below were more rapid when compared to the solidification rate at much higher laser power. The slower solidification rate at these higher laser powers promotes the formation of more

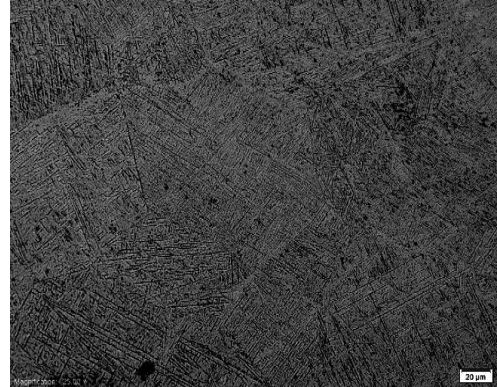
Widmanstätten microstructure as shown in Figure 14. The large quantity of the Widmanstätten (basket woven) alpha structure which is softer than the martensitic structure is responsible for the the lower microhardness observed at higher laser power.



(a)



(b)



(c)

Figure 12: The microstructure of the heat affected zone of (a) sample A (b) sample C and (c) sample G (upper part showing part of the fusion zone)

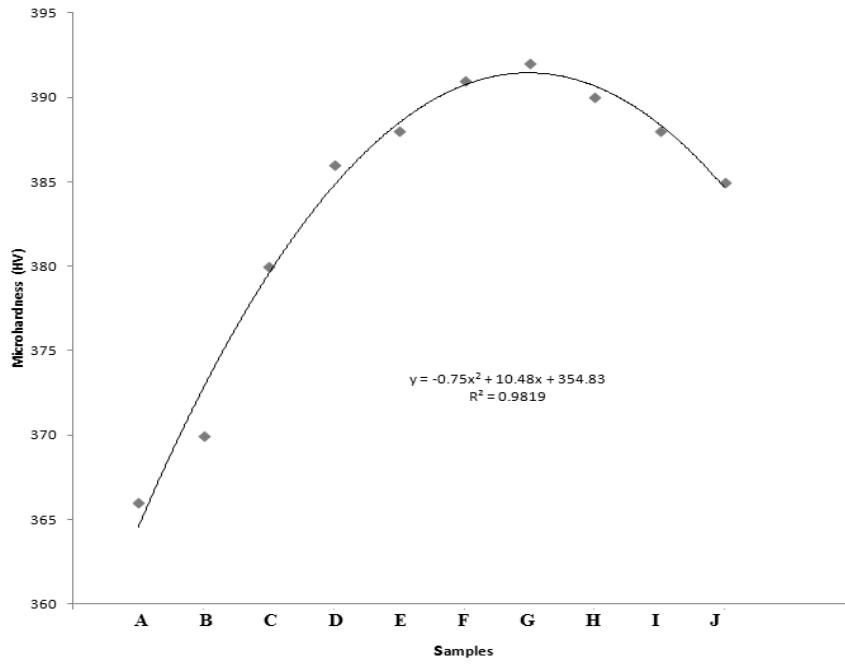
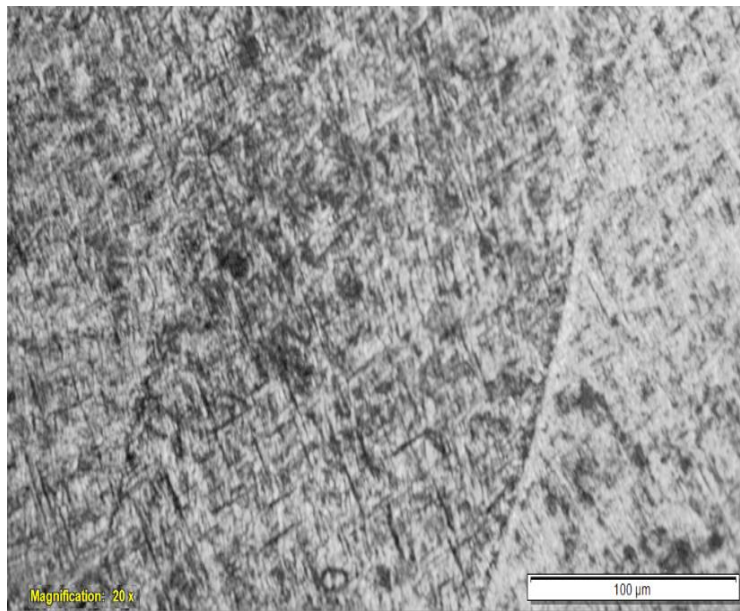
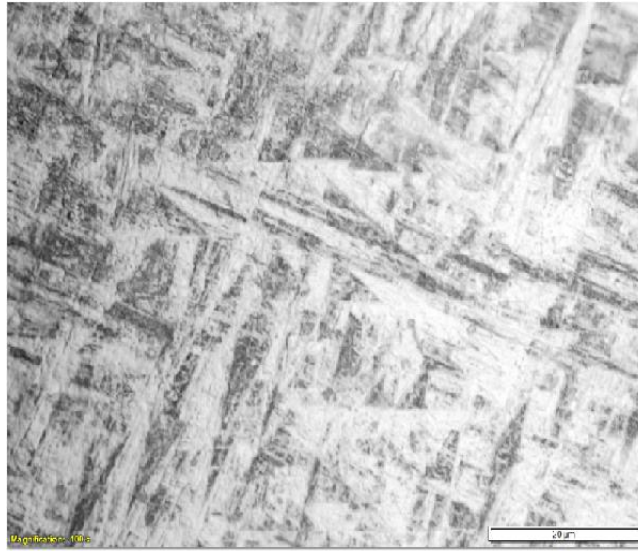


Figure 13: The plot of average microhardness value of the samples



(a)



(b)

Figure 14: (a) Microstructure of the sample J
(b) at higher magnification showing the Widmanstätten structures

4. CONCLUSION

Ti-6Al-4V has been deposited on Ti-6Al-4V substrate. The laser power was varied between 0.8 and 4.0 kW while the scanning speed, powder feed rate and the gas flow rate were kept at 0.005 m/sec, 1.44 g/min and 4 l/min respectively. The effect of changing laser power on the macrostructure, microstructure and the micro-hardness were studied. It can be concluded from the experimental results that:

1. Layer band occurred in all the samples deposited at 3 kW laser power and below, which is characterized by multi-layer deposition.
2. Microstructure of the heat affected zone changed from fine to coarse globular primary alpha grain structures with increase in laser power.
3. A range between high (at low laser power) and low density of columnar prior beta grain structure (at high laser power) were present and observed in all the samples.
4. Average micro-hardness initially increase with increase in laser power, and then decrease as the laser power was increased above 3 kW.
5. The microstructure ranges between fine martensite to thick martensite and Widmanstätten structures.

5. ACKNOWLEDGEMENT

This research work was supported by center for scientific and industrial research, national laser centre (CSIR-NLC), rental pool grant, Pretoria South Africa. This work is a revised version of oral presentation made in Hong Kong, at IMECS 2013.

6. REFERENCES

- Bergan, P., (2000). "Implementation of laser repair processes for navy aluminum components" *Proceeding of Diminishing Manufacturing Sources and Material Shortages Conference, (DMSMS)*, available at: <http://smaplab.ri.uah.edu/Smaptest/Conferences/dmsms2K/papers/decamp.pdf>, accessed on 17th June 2012.
- Brandl, E., Michailov, V., Viehweger, B., Leyens, C., (2011). "Deposition of Ti-6Al-4V using laser and wire, part I: microstructural properties of single beads" *Surface & Coatings Technology* 206: 1120–1129.
- Cai Z., Nakajima H., Woldu M., Berglund A., Bergman M, and Okabe T. (1999). "In vitro corrosion resistance of titanium made using different fabrication methods" *Biomaterials* 20(2): 183-190.
- Cottam, R. and Brandt, M., (2011). "Laser cladding of ti-6al-4v powder on Ti-6Al-4V substrate: effect of laser cladding parameters on microstructure" *Physics Procedia* 12: 323–329.
- Esmailian, M. and Mehrvar, M. (2007). "Investigation of the effect of AL₂O₃ powder in electro discharge machining for titanium alloys" *ICME*, 9: 549-557.
- Kobryn, P. and Semiatin, S.L., (2000). "Laser forming of Ti-6Al-4V: research overview" *Solid Freeform Fabrication Proceedings*, 58–65.
- Kobryn, P.A., and Semiatin, S.L, (2003). "Microstructure and texture evolution during solidification processing of Ti-6Al-4V" *Journal of Materials Processing Technology* 135(2–3): 330–339.
- Kou, S., (1987). *Welding Metallurgy*, John Wiley & Sons, New York.
- Lu, Y., Tang, H.B., Fang, Y.L., Liu, D., and Wang, H.M. (2012). "Microstructure evolution of sub-critical annealed laser deposited Ti-6Al-4V alloy" *Materials and Design* 37: 56–63.
- Mahamood, R. M., Akinlabi, E. T., Shukla M. and Pityana, S. (2012). "Functionally graded material: an overview" *Lecture Note in Engineering WCE 2012* 3: 1593-1597.

- Mahamood, R.M., Akinlabi, E.T., Shukla, M. and Pityana, S. (2013a). "Material efficiency of laser metal deposited ti6al4v: effect of laser power" Engineering Letters, 21:1, EL_21_1_03, available online at http://www.engineeringletters.com/issues_v21/issue_1/EL_21_1_03.pdf
- Mahamood, R.M., Akinlabi, E.T., Shukla, M. and Pityana, S. (2013b). "laser metal deposition of Ti6Al4V: a study on the effect of laser power on microstructure and microhardness". International Multi-conference of Engineering and Computer Science (IMECS 2013) 994-999.
- Mahamood, R.M., Akinlabi, E.T. and Akinlabi, S. A. (2014). "Laser power and scanning speed influence on the mechanical property of laser metal deposited titanium-alloy" Lasers in Manufacturing and Materials Processing 2(1): 43-55.
- R.M. Mahamood, and E.T. Akinlabi, (2016). "Process parameters optimization for material deposition efficiency in laser metal deposited titanium alloy" Lasers in Manufacturing and Materials Processing 3(1): 9-21.
- Matthew, J. and Donachie, Jr. (1988). *TITANIUM: A Technical Guide*. Metals Park, OH: ASM International.
- Mazumder J and Song L. (2010). *Advances in direct metal deposition, a laser workshop on laser based manufacturing*, University of Michigan, available at <http://www.seas.virginia.edu/research/lam/pdfs/speaker%20presentations/Mazumder-NSF-IUCRC%20workshop-2010.pdf>, accessed online on 26th August 2011.
- Messler Jr., R.W., (1999). *Principles of Welding: Processes, Physics, Chemistry, and Metallurgy*, WILEY-VCH, Weinheim.
- Peters, M., Kumpfert, J., Ward, C.H., and Leyens, C. (2003). "Titanium alloys for aerospace applications" In: *Titanium and Titanium Alloys Advanced Engineering Materials* 5: 419-427.
- Pinkerton, A. J., Wang, W. and Li, L., (2008). "Component repair using laser direct metal deposition" Proc. IMechE Part B: J. Engineering Manufacture 222: 827-836.
- Toyserkani, E. and Khajepour, A. (2006). "A mechatronics approach to laser powder deposition process" Mechatronics 16(10): 631-641.
- Wang Z.M, and Ezugwu E.O. (1997). "Titanium alloys and their machinability a review" Journal of Materials Processing Technology 68: 262-270.
- Wu, X.H., Jing, L., Mei, J.F., Mitchell, C., Goodwin, P.S. and Voice W. (2004). "Microstructures of laser-deposited Ti-6Al-4V" Materials and Design 25: 137-44.